ROLE OF PERK IN ANCHORAGE- INDEPENDENT GROWTH OF COLORECTAL CARCINOMA AND CELL MIGRATION IN-VITRO

Madhura Shirish Shukla

Submitted to the faculty of the University Graduate School
in partial fulfillment of the requirements
for the degree
Master of Science
in the Department of Biochemistry and Molecular Biology,
Indiana University

September 2020

Accepted by the Graduate Faculty of Indiana University, in partial fulfillment of the requirements for the degree of Master of Science.

Master's Thesis Committee

_____

Ronald C. Wek, PhD, Chair

_____

Lawrence A. Quilliam, PhD

_____

Mark G. Goebl, PhD

ACKNOWLEDGEMENT

I would like to express my deepest gratitude to my mentor Dr. Ronald Wek, for giving me this opportunity to prove myself in graduate school. He has been very understanding and considerate throughout the journey and has structured my learning curve while constantly pushing me to be a better researcher. I am sure all his advice will help me succeed throughout my career.

I would like to thank Dr. Lawrence Quilliam and Dr. Mark Goebl for providing me with advice whenever required. Their classes were instrumental in laying conceptual foundations for my project. Thank you for being a valuable part of my thesis committee and helping me reach my goal.

I would like to express my gratitude to Dr. Kirk Staschke with whom I have worked for the most of my time at the Wek lab. Kirk was very actively involved in my project since the very beginning, patiently answering the smallest of my doubts. He was a constant source of help, guidance, and motivation without whom this project would not be completed.

Lab members Sheree, Parth, Kenny, Leo, Jagannath and Ricardo have been very kind and helpful since my very first day at the Wek lab. From advice on experiments to discussions on food, they have always kept me good company and I would have been lost without them.

Last but not the least, I would like to thank my family, for supporting me throughout my degree till the date, encouraging me through difficult times and for always believing in me. I am thankful to my friends for keeping my life cheerful.

Madhura Shirish Shukla

ROLE OF PERK IN ANCHORAGE- INDEPENDENT GROWTH OF COLORECTAL CARCINOMA AND CELL MIGRATION IN-VITRO

The unfolded protein response (UPR) is important for cell adaptation to accumulation of unfolded proteins in the endoplasmic reticulum (ER). A central UPR sensor of ER stress is PKR- like ER Kinase (PERK), which phosphorylates eIF2 to reduce global translation and help mitigate ER stress. While this is a survival mechanism that serves to save the cell from catastrophic events during ER stress, PERK can also be activated in cancer cells due to genetic changes and exposure to stresses inherent in the tumor micro-environment. Published reports have indicated that PERK is activated in cancer cells in response to hypoxia, nutrient deprivation, matrix detachment, and increased protein load by oncogene activation to facilitate cell survival. The UPR features PERK and another ER stress sensory protein, IRE1α, which also regulates the dynamic assembly of the actin cytoskeleton; loss of either PERK or IRE1α functions decrease cell migration activity. We hypothesized that PERK is required for anchorage-independent survival of the cancer cell line HCT116 and that PERK is essential for cell migration. Consistent with these premises, inhibition of PERK using pharmacological inhibitors GSK2656157 and LY-4 in suspended cells showed reduced growth. Furthermore, PERK-deficient cells showed reduced migration in transwell migration assays as compared to their wild type counterpart. These results suggest that PERK facilitates anchorage-independent growth of cancer cells and cell migration.

Ronald C. Wek, PhD, Chair

TABLE OF CONTENTS

LIST OF TABLES

LIST OF FIGURES

LIST OF ABBREVIATIONS

Ab: Antibody

ATF4: Activating Transcription Factor 4

ATF6: Activating Transcription Factor 6

BSA: Bovine Serum Albumin

BSL2: Biosafety Level 2

bZIP: Basic Leucine Zipper

CHOP: C/EBP- homologous protein

DAG: Diacyl glycerol

DAPI: 4′,6-diamidino-2-phenylindole, Fluorescent Stain

DMEM: Dulbecco's Modified Eagle Medium

DMSO: Dimethyl sulfoxide

DNA: Deoxyribonucleic Acid

ECL: Enhanced Chemiluminescence

ECM: Extracellular Matrix

eIF2: Eukaryotic Initiation Factor 2

eIF2B: Eukaryotic initiation Factor 2B (Guanine nucleotide exchange factor for eIF2B)

eIF2α-p: Phosphorylation of the α Subunit of eIF2 at Serine 51

ERSE: ER Stress response Elements

EMT: Epithelial–Mesenchymal Transition

ER: Endoplasmic Reticulum

ERAD: Endoplasmic Reticulum Associated Degradation

FBS: Fetal Bovine Serum

FOXO: Forehead box O protein

GADD34: Growth arrest and DNA damage inducible 34 protein

GCN2: General Control Nonderepressible 2

GDP: Guanosine Diphosphate

GTP: Guanosine Triphosphate

HER2: Human Epidermal Growth Factor Receptor 2

HF: Halofuginone

HRI: Heme Regulated Inhibitor

HRP: Horseradish Peroxidase

IBTK: Inhibitor of Bruton Tyrosine Kinase

IgG: Immunoglobulin G

IRE1: Inositol Requiring Enzyme 1

ISR: Integrated Stress Response

KO: Knock Out

MET: Mesenchymal- Epithelial Transition

Met-tRNA$_i^{Met}$: Initiator Methionine Transfer RNA

mRNA: Messenger Ribonucleic Acid

MRP1: Multidrug Resistance Related Protein

MW: Molecular Weight

NRF2: Nuclear Factor Erythroid 2–Related Factor 2

PBS: Phosphate Buffer Saline

PFA: Paraformaldehyde

PERK: PKR-like ER Kinase

PET: Polyester

PKR: Protein Kinase R

Poly-HEMA: Poly-2-Hydroxyethyl Methacrylate

PP1c: Type 1 Protein Phosphatase Complex

ROS: Reactive Oxygen Species

RPM: Revolutions Per Minute

SDS: Sodium Dodecyl Sulfate

SEM: Standard Error of Mean

SERCA: Sarco/Endoplasmic Reticulum Calcium ATPase

TBST: Tris Buffer Saline with 0.1% Tween 20

Tp: Thapsigargin

tRNA: Transfer Ribonucleic Acid

uORF: Upstream Open Reading Frames

UPR: Unfolded Protein Response

UV: Ultraviolet

WT: Wild Type

XBP1: X-box binding protein

INTRODUCTION

Disruption of ER homeostasis leads to activation of the unfolded protein response

The endoplasmic reticulum (ER) is a system of membranous tubules that is central for synthesis, folding, assembly, and transport of proteins designated for the secretory pathway. Furthermore, the ER is central for calcium storage and release and for lipid synthesis. Chaperones localized in the ER participate in protein folding and assembly and there is further post-translational modification of newly synthesized proteins in this organelle. Misfolded proteins are detrimental to the cell and therefore need to be appropriately eliminated. When there is accumulation of unfolded proteins in the ER, it disrupts protein homeostasis and leads to ER stress. Terminally misfolded proteins are subjected to degradation via ER associated degradation (ERAD) pathway.

In addition to conditions directly linked to misfolded proteins, ER stress is caused by genomic instability, hypoxia, changes in temperature, and reactive oxygen species (ROS) (1-5). Pharmacological agents, such as thapsigargin (Tp), can induce ER stress. Thapsigargin blocks the calcium pump Sarco/Endoplasmic Reticulum Calcium ATPase (SERCA) in the ER, resulting in rapid release of Ca^{2+} from the ER. Calcium depletion from the ER leads to loss of activity of calcium dependent chaperones in the ER that triggers accumulation of unfolded proteins and ultimately ER stress (6,7). Another pharmacological agent that induces ER stress is tunicamycin, which thwarts N-glycosylation in the ER and consequently prevents appropriate modification of secreted proteins.

Accumulation of misfolded proteins activate one of the three ER stress sensors: PKR-like ER Kinase (PERK), Activating Transcription Factor 6 (ATF6), and Inositol Requiring Enzyme 1 (IRE1). Collectively, the signaling response mounted by these ER stress sensors is referred to as the Unfolded Protein Response (UPR). It is suggested that under non-stressed conditions, these ER transmembrane proteins are bound by the chaperone BiP (GRP78, HSPA5) and thus remain inactive. But accumulation of misfolded proteins competes for BiP binding to these sensory proteins, leading to release of the chaperon. Upon the release of BiP, PERK and IRE1α dimerize, triggering autophosphorylation that contributes to their activation (1,8-10). Additional models of activation suggest that IRE1α and PERK can be directly bound to unfolded protein that accumulate during ER stress, leading to their autophosphorylation and enhanced signaling (11,12).

IRE1α possesses protein kinase and riboendonuclease activities. Upon activation, IRE1α riboendonuclease directs the cleavage and removal of a segment of X-box binding protein 1 *(XBP1)* mRNA, and the remaining portion of the transcript is ligated by a tRNA ligase RTCB (13). The cytosolic splicing of the *XBP1* transcript leads to translation of an active basic leucine zipper (bZIP) transcription factor that enters the nucleus and binds to ER stress response elements (ERSE) in the target promoters of UPR genes. ATF6 is another bZIP transcription factor that upon ER stress is transported to the Golgi apparatus, where ATF6 is cleaved via S1 and S2 proteases, leading to release of an amino terminal portion of ATF6, designated ATF6(N), that is released from the Golgi into the cytosol. ATF6(N) then enters the nucleus to induce the transcriptional expression of UPR genes (1,7,14).

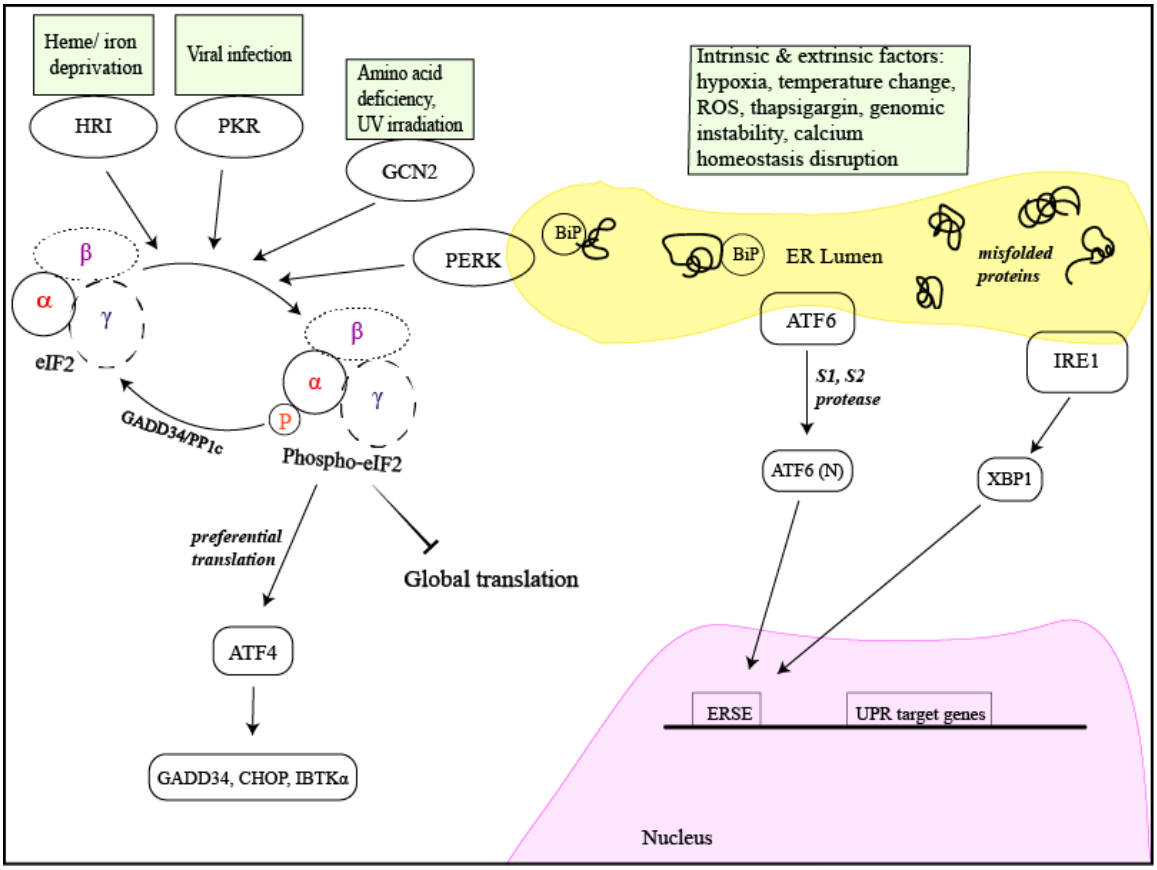

Figure 1: Depiction of activation and cascade of various stress sensors of UPR and ISR

Different intrinsic and extrinsic cell stresses cause accumulation of misfolded proteins in the endoplasmic reticulum leading to stress of this organelle. Three ER transmembrane proteins, PERK, ATF6, and IRE1α, monitor perturbations in the ER lumen and membrane. Sensing of the ER stress is suggested to involve release of inhibitory interactions with an ER chaperone, BiP. Activation of IRE1α and ATF6 leads to induction of bZIP transcription factors XBP1 and ATF6(N), respectively. These ER sensors upregulate the transcription of UPR-target genes to mitigate stress damage. Four eIF2 kinases, GCN2, PERK, HRI, PKR, are activated by different cellular stresses, leading to phosphorylation of the α subunit of eIF2 at serine 51 (eIF2α-P).

Phosphorylation of this translation initiation factor reduces global protein synthesis accompanied by preferential translation of gene transcripts required to adapt to the stress.

The third ER stress sensor PERK is a serine/threonine kinase that phosphorylates the α subunit of eukaryotic initiation factor 2 (eIF2α) at serine-51 to regulate translation control in the UPR (15,16). PERK has also been reported to also phosphorylate nuclear factor erythroid 2–related factor 2 (NRF2), Diacyl glycerol (DAG), and Forehead box O protein (FOXO) (17-19), although these signaling processes have not been extensively studied.

Global translation repression and preferential translation of stress adaptive genes reinstate ER homeostasis

One of the major substrates of PERK is eIF2, which binds to GTP and delivers initiator methionyl tRNA (Met-$tRNA_i^{Met}$) to the 40S ribosome for initiation of mRNA translation. During the translation initiation process, the GTP associated with eIF2 is hydrolysed to GDP. The GDP on eIF2 must then be exchanged for GTP by the guanine nucleotide exchange factor eIF2B, for the further translation initiation. During ER stress, PERK phosphorylation of eIF2α thwarts the eIF2B-directed exchange, sharply lowering the levels of eIF2-GTP that results in reduced delivery of initiator tRNA to ribosomes. The resulting reduction in global protein synthesis lowers energy and nutrient expenditure, facilitating cell adaptation to the underlying stress. Additional eIF2 kinases in mammalian cells include General Control Nonderepressible 2 (GCN2), Heme Regulated Inhibitor (HRI) and Protein Kinase R (PKR) (10,20). GCN2 is induced during

nutrient deprivation (9,20) and in response to UV irradiation (21). HRI is activated in reticulocyte cells in response to heme or iron deprivation (22) and mitochondrial stress (23,24), whereas PKR is activated by viral infections (25). In addition to accumulating misfolded proteins, disruption of calcium homeostasis and lipid synthesis can also cause ER stress that enhances PERK eIF2 kinase activity (1,10). Phosphorylation of eIF2α represses global translation initiation in the cell coincident with enhanced preferential translation of certain genes involved in transcription, protein turnover, and cell cycle. Because the four different eIF2 kinases regulate translation in response to diverse stress, this pathway is collectively referred to as the Integrated Stress Response (26).

In mammals, eIF2α-P is well documented to enhance translation of Activating Transcription Factor 4 (ATF4), a bZIP transcription factor. Translation of *ATF4* involves upstream open reading frames (uORFs) present in the 5'-leader of its gene transcript; preferential translation of *ATF4* upon eIF2α phosphorylation by a mechanism of delayed translation reinitiation (27). Increased levels of ATF4 protein then direct target promoters of ISR genes, including those encoding C/EBP- homologous protein (CHOP), Growth arrest and DNA damage inducible 34 (GADD34) protein, and Inhibitor of Bruton Tyrosine Kinase (IBTKα), each of which are also subject to preferential translation (28-30). CHOP is a bZIP transcription factor responsible for apoptotic cell fate and its mRNA is also preferentially translated by a mechanism involving an uORF (31). GADD34 is a scaffolding protein, which is induced by both transcriptional and translational mechanisms in the ISR (32-34). GADD34 forms a complex with type 1 protein phosphatase complex (PP1c) and dephosphorylates eIF2α (29,35-37). Taken together,

PERK integrates the UPR and ISR in order to alleviate disruptions in protein homeostasis and restore the health of the ER.

Role of PERK in cancer

Cancer cells face a multitude of intrinsic and extrinsic stresses, many of which directly or indirectly disrupt the functions of the ER. A major intrinsic perturbation in cancers is genome instability. An example is in chronic myeloid leukemia that features a chromosome translocation that produces BCR-ABL1, an active oncoprotein. Production of this oncoprotein disrupts ER homeostasis and ER-mediated calcium-dependent apoptotic responses (1,38). Furthermore, amplification of *Myc* oncogene facilitates cell growth and proliferation involving increased ribosome production and increased mRNA translation. Enhanced protein synthesis can overwhelm the protein folding machinery, leading to ER stress and PERK activation. The ensuing stress response helps cancer cells adapt to Myc induction and other external stresses encountered by the cell. Activation of PERK has been reported in a number of other cancers, including lymphomas and those affecting the prostate (39-41).

Extrinsic stresses involving hypoxia, glucose and nutrient deprivation, and ROS accumulation occur in tumor microenvironment, triggering ER stress (1,39). Hypoxia leads to PERK activation, which helps tumor cells to adapt to the oxygen depletion; loss of PERK can lead to apoptosis of cancer cells in hypoxic environments and reduction of tumor size (42,43). It was also reported that in breast adenocarcinoma cells, PERK and ATF4 are essential for cell migration in hypoxia and loss of these stress adaptive genes

reduce migration in-vitro (44). PERK is important for alleviating ROS production, which can elicit DNA damage (45). Apart from intrinsic and extrinsic factors inherent in cancer cells proliferation and progression, PERK also plays a role in cancer cell survival against chemotherapeutic agents by upregulating multidrug resistance related protein (MPR1) via a pathway involving PERK induction of NRF2, as reported by Salaroglio I. C. et al (46).

Resistance of anoikis in cancer

Anoikis is a form of apoptotic cell death that is triggered upon detachment of cells from the extracellular matrix. Some normal migratory cells, such as leukocytes, are protected from anoikis due to their amoeboid migration (47). ECM detachment and migration are primary steps leading to metastasis, and this process requires cancer cells to be resistant to anoikis. When cells detach from ECM, the apoptotic pathway is triggered due to the absence of pro-survival responses provided with cell-ECM interactions (48,49). PERK induces autophagic responses during matrix detachment in breast cancer cells and this eIF2 kinase promotes antioxidant responses against ROS to protect the cells from anoikis (50).

Cell Migration and UPR

Cell migration is an important phenomenon in cancer progression. The role of cell migration in metastasis process involves three critical steps: 1) detachment of tumor cells from the original site of the tumor, 2) survival of the cancer cells during anchorage-independence, and 3) cancer cell reattachment at a new metastatic site. Cancer cells detach as single cell or in clumps of cells. Detachment involves cytoskeleton changes as a

part of epithelial–mesenchymal transition (EMT) and entrance of cancer cells into the blood stream. Initiation of migration requires changes in polarity of the cells to form a leading edge and polarity is achieved by remodelling of the actin cytoskeleton. After survival through the anchorage-independence through the blood stream, the cancer cell attaches to the secondary site by reverse process of EMT: mesenchymal- epithelial transition (MET) (51,52). Various stresses are experienced by cancer cells during migration and metastasis, which can activate the UPR pathway to mitigate stress damage. For example, expression of ATF4 is enhanced by HER2 overexpression in breast cancer cells and increased levels of ATF4 are suggested to promote cell migration by inhibiting E-cadherin expression (53). In some types of cancers, UPR activators PERK and IRE1α are shown to drive cell migration in response to hypoxia and ER stress inducing conditions via ATF4 and XBP1 (44,54,55).

In a normal epithelial cell, cortical distribution of F-actin maintains cell shape, but upon receiving a migratory stimulus, actin stress fibers are formed to project filopodia and lamellipodia for cell migration (56,57). Both IRE1α and PERK are suggested to contribute to the dynamics of the actin cytoskeleton. IRE1α interaction activates filamin A, a key factor in actin polymerization, to cause actin remodelling via Rho GTPase. IRE1α deficient cells showed fewer filopodia and lamellipodia protrusions that contribute to reduced migration suggesting that IRE1α is required for cell migration (58). PERK also associates with filamin A and causes cortical F-actin distribution that affects cell migration in a wound closure assay (59). It is noteworthy that the enzymatic activities of IRE1α and PERK are dispensable for actin remodelling, emphasizing that these UPR

sensory proteins can serve as scaffolding proteins for complex signalling networks.

Questions addressed in this thesis

The aim of this study is to address the role of PERK in cancer progression, specifically in in cancer cell migration and anchorage-independent growth. Three questions are addressed: Does matrix detachment cause ER stress in colorectal cancer cells and attendant induction of the UPR? What role does the UPR play in anchorage-independent survival and growth of the cancer cells? Finally, what function does PERK play in cell migration? Addressing these critical questions is important to provide new insights into the mechanisms by which the UPR contributes to cancer metastasis.

MATERIALS AND METHODS

Cell culture

The human colorectal adenocarcinoma cell line, HCT116 (ATCC, CCL-24) was cultured in 1X McCoy's 5A (modified) media containing 0.22 g/L L-Glutamine (Sigma Aldrich, M4892) that was supplemented with 10% FBS and 2.2g/L sodium bicarbonate. Cells were cultured until 70-80% confluency and fed every 2-3 days. Freezer stocks of the HCT116 cells were prepared in 1X McCoy's 5A+ 20% FBS+ 5% DMSO and stored in liquid nitrogen. 2X media for soft agar assays was prepared from powdered McCoy's 5A media (Sigma Aldrich, M4892) supplemented with 4.4 g/L sodium bicarbonate and 20% FBS.

Mouse embryonic fibroblast (MEF) cells (60) were cultured in 1X Dulbecco's Modified Eagle's Medium (DMEM) (Fisher Scientific, MT10013CV) supplemented with 10% FBS. The cells were passaged until 70-80% confluency. Fresh media was added to the cultures every 2-3 days. Freezer stocks were prepared in 1X DMEM+ 20%FBS+ 10% DMSO and stored in liquid nitrogen. *PERK*$^{-/-}$ MEF cells were isolated from embryos from PERK knock-out animals as described in Jiang H.Y. et al (60).

To facilitate cell passage, cells were trypsinized using TrypLE express (Fisher Scientific, 12605-010) for 5-7 minutes at 37^{o}C. Cell counting was performed by mixing 10 µL of cell suspension and 10µL of 0.4% Trypan blue. 10µL of this mixture was applied onto counting slides and inserted into TC20 automated cell counter (Bio-Rad,

1450102). The unstained cells in the size range of 8-25 µm were counted as live cells. Live cell count was used to seed cells for tumor sphere and migration assays.

Preparation and quantification of protein lysates

Lysate preparation from adherent cells

Cells were plated in 6-well plates for overnight growth. The next day, sub-confluent cells were removed using a sterile cell scraper, collected by centrifugation, and washed twice with 5 mL of 1X PBS. Lysates were prepared in 80 µL 1% SDS lysis solution supplemented with 1X protease and phosphatase inhibitor cocktail (Thermo Fisher; 78444). Whole cell lysates were incubated at 95^{o}C for 5 minutes and then cells were subjected to 15 pulses of sonication using a VWR Branson 450 Sonifier with Probe at timer 0.2, duty cycle 20%, output control 4. Lysates were clarified by centrifugation at 12000 RPM for 15 minutes at room temperature in an Eppendorf 5424 centrifuge. Clarified supernatants were transferred to a fresh microfuge tube and used for protein quantification using a Bradford Bio-Rad DC protein assay, which involves a colorimetric protein determination using Coomassie blue. Absorbance was measured at 750 nm and the concentration of each lysate was determined by using bovine serum albumin (BSA) standards ranging from 0.2- 1.0 mg/mL (Bio-Rad).

Lysates preparation from non-adherent spheres

Cultured spheres that were suspended in growth media were collected into a sterile 15 mL Falcon conical centrifuge tube and subjected to centrifugation at 200 x g for 5 minutes at room temperature in an Eppendorf 5810R centrifuge. The media was

removed, and the collected spheres were washed twice in 1X PBS solution and lysed using 80 µL 1% SDS solution supplemented with 1X protease and phosphatase inhibitor cocktail (Thermo Fisher; 78444). Lysates were incubated at 95^{o}C for 5 minutes and the cell preparation was subject to sonication for 15 pulses using VWR Branson 450 Sonifier with Probe at timer 0.2, duty cycle 20%, output control 4. Lysates were clarified by centrifugation at 12000 RPM for 15 minutes at room temperature in Eppendorf 5424 centrifuge. Clarified supernatants were transferred to a fresh tube and used for protein quantification. Protein quantification of all lysates was done using the Bio-Rad DC protein assay.

SDS-PAGE and western blot analysis

4X laemmli sample buffer solution was prepared by mixing 900 µL of 4X laemmli buffer stock (Bio-Rad; 161-0747) with 100 µL of β-mercaptoethanol. 4X laemmli sample buffer solution (5µL) and SDS lysis buffer were mixed with 20 µg of protein sample in total 20 µL volume. Samples were boiled for 5 minutes and proteins were separated by electrophoresis in a 10% TGX stain-free FastCast acrylamide gel (Bio-Rad; 161-0173) using 1X SDS running buffer for 1.5 h at 90-120 volts. Precision Plus Dual color protein standards (Bio-Rad; 1610374) were used with each gel to delineate protein molecular weights.

Separated proteins were transferred to nitrocellulose membranes using a Bio-Rad TransBlot machine and TransBlot transfer buffer solution at a current of 1.3A, up to 25V for 10 minutes. The proteins bound to membranes were incubated with 5% blocking

grade milk (Bio-Rad; 1706404**)** in 1X TBST for 1 h at room temperature. Primary antibodies for target proteins were then added, followed by incubation overnight in a solution of 5% blocking grade milk at 4^{o}C with gentle rocking. The membranes were then washed three times for 10 minutes each with a 1X TBST buffer solution. HRP-conjugated secondary antibody complementary to the primary antibody was diluted 1:5000 in 5% blocking grade milk solution and incubated for 1 h at room temperature with mixing. A list of primary and secondary antibodies, their dilutions used in experiments, and their description are provided in Table 1. ATF4 and phospho-PERK antibodies were made as described by Teske B. F et al and Tenkerian C. et al, respectively (61,62). Membranes were washed with 3 times with 1X TBST solution, each for 10 minutes, to remove unbound antibody from the membranes and protein bands were detected using ECL-enhanced chemiluminescence reagents (Bio-Rad; 1705060). Images of chemiluminescent protein bands and colorimetric protein ladders were captured using ‘optimal auto exposure’ in the Bio-Rad ChemiDoc imaging system. Chemiluminescent and colorimetric images were superimposed to note the relative positions of protein bands and the protein standard ladder.

Table 1: List of antibodies and their dilutions used in western blot analysis

List of primary antibodies used for western blot analysis to detect ATF4, beta-actin, GADD34, phospho-eIF2, phospho-GCN2, phospho-PERK, total eIF2 and total PERK used at their standard dilution. The secondary antibodies against rabbit or mouse were used at 1:5000 dilution and were detected using HRP-conjugated ECL reagents.

Protein detected	**Dilution**	**Type**	**Source**
ATF4	1:5000	Rabbit, primary Ab	Original (61)
Beta-Actin	1:5000	Mouse, primary Ab	Sigma-Aldrich, A5441
GADD34	1:500	Rabbit, primary Ab	ProteinTech,10449-1-AP
Goat Anti-Mouse	1:5000	HRP conjugate IgG	Bio-Rad, 170-6515
Goat Anti-Rabbit	1:5000	HRP conjugate IgG	Bio-Rad, 1721019
Phospho-eIF2 (Ser 51)	1:500	Rabbit, primary Ab	Abcam, Ab32157
Phospho-GCN2	1:500	Rabbit, primary Ab	Abcam, Ab75836
Phospho-PERK	1:500	Rabbit, primary Ab	Original (62)
Total eIF2	1:3000	Rabbit, primary Ab	Cell Signaling Technology, D7D3 XP^{R}
Total PERK	1:500	Rabbit, primary Ab	Cell Signaling Technology, C33E10

Formation of tumor spheres

Using poly-HEMA coated plates

To determine the function of PERK in anchorage- independent growth, we used culture plates coated with poly-HEMA which inhibit the attachment of cells to the culture plate, causing cells to remain suspended (63,64). This coating method allowed for easy isolation of protein lysate as compared to matrix-based 3D cultures. The poly-HEMA stock was prepared using poly-2-hydroxyethyl methacrylate (Aldrich, 192066) in the following protocol: 2g of poly-HEMA powder was added to a final volume of 100 mL of 95% ethyl alcohol in a sterile bottle. The solution was prepared by heating at 65^{o}C and mixing using a sterile stir bar and mixing plate until the HEMA powder was fully

dissolved into the solution. Poly-HEMA solution (4 mL) was added per 10 cm dish ensuring uniform distribution over the surface of the plate. Plates were kept open overnight at room temperature for drying using sterile technique inside of a biosafety cabinet. HCT116 cells were then washed with 1X PBS, trypsinized and mixed with normal growth media to prepare a single cell suspension. A sample of 10^5 cells were seeded onto each 10 cm cell culture dish coated with poly-HEMA and the plates were incubated at 37^{o}C in 5% CO_2 incubator for 15 days to allow sphere formation.

Soft agar assay

Soft agar assays were performed in 12-well plates that were coated with 500 µL/well of poly-HEMA stock and dried. A 0.7% agar solution was prepared and sterilized to be used as matrix and 300 µL of the solution was added onto the poly-HEMA coated surface to make 'base agar layer'. Parental HCT116 cells were washed with a 1X PBS solution, trypsinized and then mixed with 2X McCoy's 5A media to make a single-cell suspension. The cell suspension was diluted with 2X media such that there were 1000 cells per 300 µL of media solution. The 300 µL of the cell/media suspension was then mixed with 300 µL of agar stock (at approximately 40^{o}C), thus making the final media concentration 1X and 0.35% agar. The agar and cells were gently mixed and added on top of the base agar layer. Once the agar solidified, 600 µL 1X normal growth media was added on top of the agar. The wells were then seeded with DMSO control, or the indicated amounts of LY-4 and GSK2656157, each with three replicates. The cultured cell assays were incubated in 37^{o}C, 5% CO_2 incubator for 14 days. Images of 5 fields per

well were taken with 10X objectives of inverted compound microscope to quantify the assay.

Transwell cell migration assay

Transwell migration was performed using 8 µm PET membrane inserts (Greiner bio-one, 662638) coated with collagen I (Corning, 354249). The collagen I solution was prepared by mixing 10.7 µL collagen I stock (9.3 mg/mL) with 990 µL 70% molecular biology grade ethanol. 50 µL of the collagen solution was added on top of the membrane, making the final collagen concentration on the membrane to be approximately 15 µg /cm^2. The coated membrane inserts were placed in 24-well plates and dried overnight. The next day, wild type MEF cells or their *PERK*$^{-/-}$ counterparts were washed with 1X PBS, trypsinized and then mixed with normal growth media. Cells were collected by centrifugation at 200 x g for 5 minutes to remove media. The cell pellet was washed with 1X PBS solution followed by centrifugation. The cells were then suspended in 1X DMEM media without FBS and cell density was determined by cell counting. 500 µL of 1X DMEM supplemented with 10% FBS was added in each well and the inserts were placed on top, making sure that the media in the bottom did not flow back inside the insert. Then 20,000 cells were added inside the filter with 200 µL of 1X DMEM without FBS. While setting up migration assay with PERK inhibitor GSK2656157, the compound was added in both, insert and the lower chamber at 2 µM. The cells were allowed to migrate for 1 h, 6 h, 12 h, or 18 h as per the setup depicted in Figure 2.

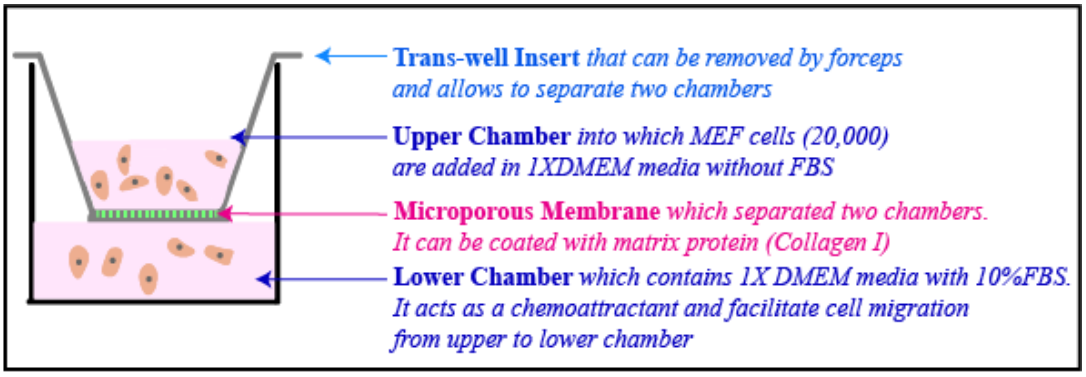

Figure 2: Arrangement of transwell migration assay

The figure depicts the arrangement of transwell migration assay. The transwell insert with collagen coated membrane separates the upper and lower chambers while allowing the cells to migrate through it. The lower chamber contains growth media with attractant (10% FBS) that facilitates cell migration. The insert is removed using forceps.

For fixing cells, 4% paraformaldehyde (PFA) solution was prepared by mixing 4 g of PFA to 50 mL 1X PBS solution with gentle stirring on heating block at 60^{o}C. Then the mixture was cooled down to room temperature and the pH was adjusted at 7.4 with 1M HCl. The final volume was made to 100mL using 1XPBS. The 4% PFA solution was filtered through 0.45 µm filter and used for fixing (or stored at -20^{o}C) membrane of transwell migration assay. After each timepoint, the inserts were removed from media and placed in 600 µL of 4% PFA in 1X PBS solution for 15 minutes. The membrane inserts were washed twice using a 600 µL 1X PBS solution for 10 minutes per wash. The fixed membranes were stored in 1X PBS solution at 4^{o}C until stained. The membranes were cut out by poking a syringe around the rim and the membrane segment was then placed in DAPI mixed with Prolong Gold Antifade reagent (Invitrogen, P36935) on slide. Equal volumes (1.5µL of each) of 75 nM DAPI working stock solution and Prolong Gold

Antifade reagent were mixed on slide. The membrane was then placed in the mixture such that the bottom of the membrane touches the slide and coverslip was placed on top. The bottom of the membrane was observed under 40X objective using a fluorescence microscope and 3 random fields of each membrane was captured to quantify migrated cells.

Assay quantification and statistical analysis

For soft agar assay, the number of spheres per field were counted manually and then averaged. The area of the sphere was measured using software ImageJ (65). Freehand circles were drawn over the border of each sphere using the 'freehand drawing' tool and then analyze> measure command gave the area of sphere marked by the circle (as represented in Figure 3). The average area was calculated from two biological replicates from a total of 90-95 spheres per treatment.

For transwell migration assays, the number of migrated cells per field were counted and averaged. The assay was seeded in duplicate per treatment per timepoint. Three random fields were captured per insert and the cell count per field was averaged from 6 fields at each timepoint. The P value was calculated using two-tailed student's T-test at $P<0.05$.

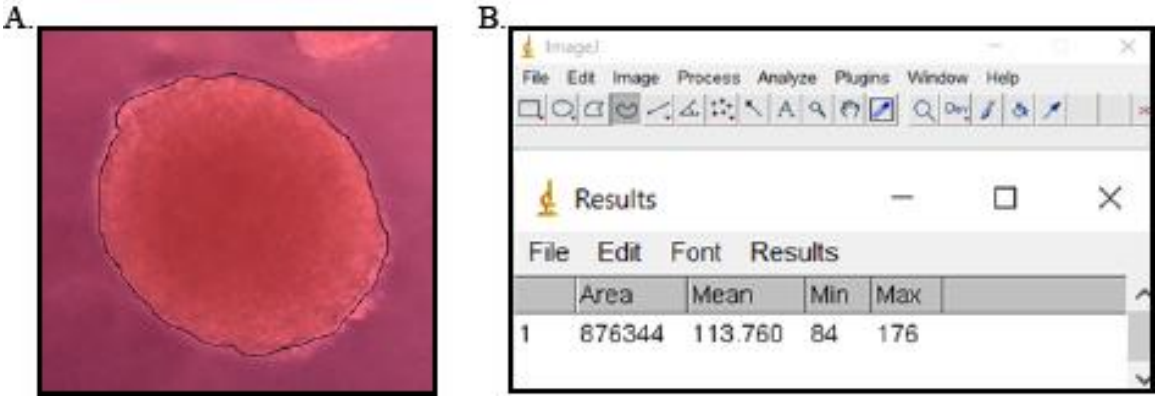

Figure 3: Measurement of sphere area from soft agar assay using ImageJ

A. Depiction of free-hand drawing of boundary surrounding the sphere to measure its area. B. The panel shows selected free hand drawing tool in ImageJ and the lower portion shows the results of the area measurement of the sphere presented in panel A.

RESULTS

Activation of PERK at late stages of sphere formation during anchorage-independent growth of colorectal carcinoma cells in vitro

PERK is reported to participate in anoikis resistance upon matrix detachment (50), suggesting that the eIF2 kinase is activated during anchorage-independent growth. To test this possibility, HCT116 cells were grown in suspension for up to 15 days and the formation of spheres was monitored by microscopy. In addition, protein lysates were prepared every third day to test for activation of the PERK and its downstream effectors. Poly-HEMA coated plates were used to facilitate anchorage-independent growth of HCT116 tumorspheres. A protein lysate at day 0 was prepared from a cell suspension prior to seeding. Cells ($1x10^5$) were seeded in 10 cm cell culture dishes as single cell suspension and the growth of tumorspheres was tracked on days 1, 3, 6, 9, 12, 15 by capturing images of five random fields. To quantify the growth of spheres over time, the sphere area of 15 to 20 spheres was measured for each timepoint and plotted. During initial suspension, the cells were clumped together (day 1) and then started forming tumorspheres at day 3 (Figures 4A and B). The growth of tumorspheres increased significantly until day 12 and reached saturation by day 12 – 15 (Figures 4A and B).

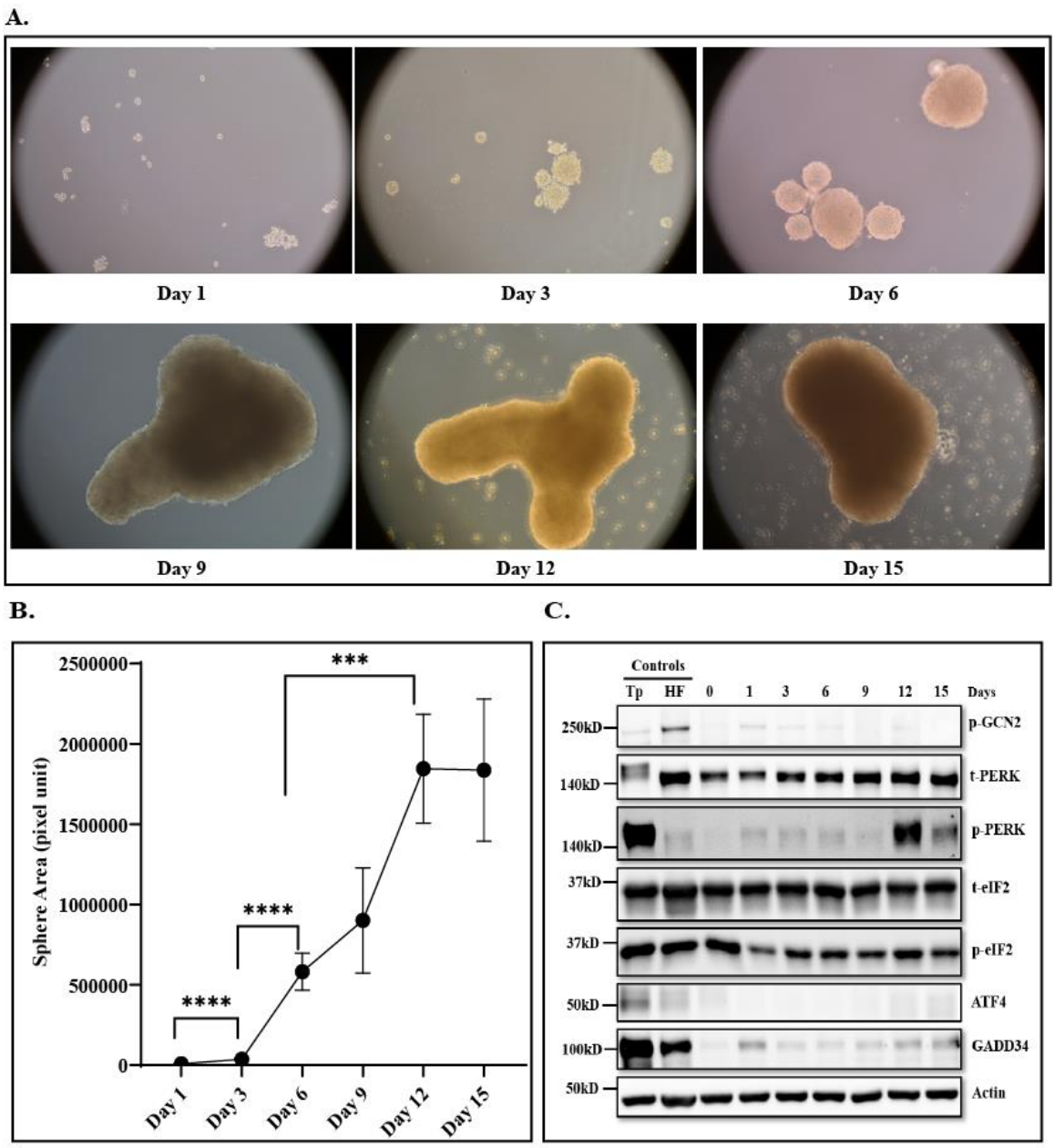

Figure 4: Anchorage-independent growth of HCT116 and PERK activation.

A. Growth of three-dimensional spheres of HCT116 cells for up to 15 days. B. Quantification of growth of spheres over 15-day period. The area of the sphere is represented as mean ± SEM. Statistical significance was determined by two-tailed student's T-test at $P<0.05$; n=15 to 20. ***$P=0.0007$, ****$P<0.0001$. C. Western blot measurements of protein biomarkers for activation of PERK pathway in response to non-

adherent conditions from day 0 to day 15. Thapsigargin treatment (Tp; 1 μM for 6 h) and halofuginone treatment (HF; 100 nM for 6 h) on normal adherent cells represent controls for PERK and GCN2 activation, respectively.

To evaluate the regulation of the key markers in the ISR we measured their total and phosphorylation levels by western blotting (Figure 4C). Controls for the experiments included treatment with thapsigargin, which is a robust inducer of ER stress and PERK activator, and halofuginone- an inhibitor of prolyl tRNA synthetase that mimics nutrient depletion and activates GCN2 (66). During the anchorage-independent growth, PERK showed modest phosphorylation during the early time course, with robust activation at the later stages, day 12 to day 15 (Figure 4C). Minimal phosphorylation of GCN2 was detected during the time course. As expected, thapsigargin induced phosphorylation of PERK but not GCN2 and halofuginone potently induced phosphorylation of GCN2. The levels of phosphorylation of eIF2α were largely unchanged during the growth period. There was a gradual increase in GADD34 throughout the course of sphere formation. The constant levels of phosphorylated eIF2 can be attributed to negative regulation by increasing levels of GADD34. The measurement of β-actin was used as a control for normalization to ensure similar levels of total protein were being analyzed. In conclusion, PERK activation occurs during the development of tumorspheres. Factors that activate PERK during late stage of sphere formation could be hypoxia or certain forms of nutrient deprivation that are selective for ER stress.

PERK inhibition by knockout or pharmacological inhibitors

To address the importance of PERK activation in HCT116 tumorsphere formation, we tested two PERK inhibitors in the soft agar assay. GSK2656157 is an established PERK inhibitor developed from previous PERK inhibitor compounds to gain higher selectivity for the ATP pocket in the kinase domain of PERK (67,68), but does have some off target affects against other protein kinases (69). LY-4 is a highly selective PERK inhibitor (70,71). To first test the utility of these inhibitors to inhibit PERK activity in HCT116 cells, we used thapsigargin to induce ER stress and PERK activation in the absence or presence of each compound.

HCT-116 cells were treated with GSK2656157, LY-4, or vehicle (DMSO) as a control for 30 minutes, followed by 1 μM thapsigargin for 4 h to induce PERK activation. Levels of PERK and eIF2α phosphorylation were measured in the treated cells by western blotting. DMSO was used as vehicle control for both PERK inhibitors. Thapsigargin treatment was done in combination with DMSO vehicle as a control for PERK activation. Halofuginone treatment was also performed as a control for GCN2 activation (Figure 5). To ensure proper normalization of protein levels, β-actin was also measured in the western blot analyses. DMSO vehicle treated cells showed increased levels of phosphorylated PERK and eIF2, and increased protein levels of their downstream targets ATF4 and GADD34 (Figure 5A). Whereas, halofuginone treated control cells did not activate PERK. Pre-treatment of HCT116 cells with either LY-4 or GSK2656157 substantially ablated the induction of phosphorylation of PERK and thwarted expression of downstream targets ATF4 and GADD34, following treatment

with thapsigargin (Figure 5A). Taken together, LY-4 and GSK2656157 compounds were confirmed to be potent PERK inhibitors in HCT116 cells.

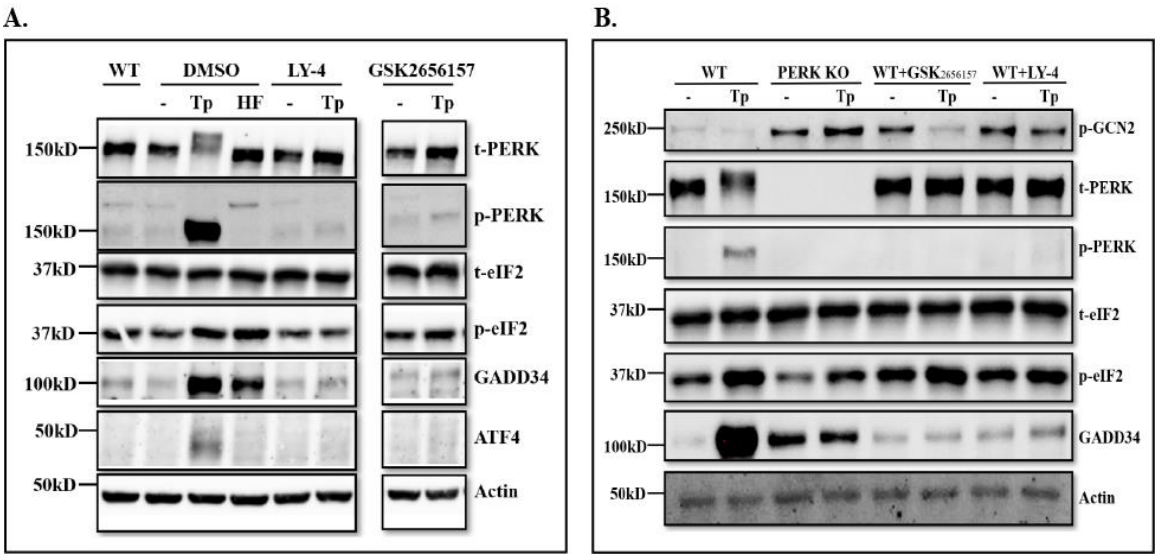

Figure 5: PERK inhibition by knockout and pharmacological inhibitors.

A. HCT116 cells were incubated with 2 µM of LY-4, GSK2656157, or DMSO vehicle 30 minutes prior to 4 h treatment with thapsigargin, as indicated. Halofuginone that selectively activated eIF2 kinase GCN2 was used as a control. Lysates were prepared, separated by SDS-PAGE, and the indicated proteins were measured by western blot analyses. Migration positions of pf of marker proteins are indicated to the left of each panel. B. Wild-type (WT) MEF cells and their PERK-KO counterparts were treated with thapsigargin as indicated and the indicated proteins were measured by western blot analyses. PERK inhibitors LY-4 and GSK2656157 were added 30 minutes prior to thapsigargin treatment. Tp= 1 µM Thapsigargin for 4 h and HF= 100 nM Halofuginone for 6 h.

We extended our analysis of the inhibitors using MEF cells. *PERK*-deleted MEF cells were reported by Jiang H.Y. et al (60) and these cells provided useful controls for our analysis of the PERK inhibitors. Wild-type and *PERK*$^{-/-}$ MEF cells were cultured to sub-confluency and treated with 1μM thapsigargin for 4 h. In wild-type cells, there was phosphorylation of PERK and eIF2 in response to the ER stress, along with enhanced levels of the downstream ISR target GADD34 (Figure 5B). PERK protein was not detected in in the *PERK*$^{-/-}$ cells, confirming the validity of our western blot analyses. However, it is noteworthy that there was some phosphorylation of eIF2 and presence of GADD34 in the PERK-deficient cells upon ER stress, although less that wild-type (Figure 5B). Cells with loss of primary eIF2 kinases have been suggested to engage alternative secondary eIF2 kinases to in part compensate (60). Consistent with this model, phosphorylation GCN2 was observed in both vehicle and thapsigargin treated *PERK*$^{-/-}$ cells but not their wild type counterparts (Figure 5B). These results suggest that phosphorylation of eIF2 and GADD34 expression may be attributed to compensatory GCN2 activation.

Next, we addressed pharmacological inhibition of PERK in the wild-type MEF cells. The *PERK*$^{+/+}$ MEF cells were pre-treated for 30 minutes with the inhibitors GSK2656157 or LY-4 followed by 4 h with thapsigargin. Cells treated with PERK inhibitors did not show PERK activation upon treatment with thapsigargin for 4 h (Figure 5B). However, phosphorylation of GCN2 was again observed with the MEF cells upon the pharmacological inhibition of PERK activity. Furthermore, phosphorylation of eIF2 and GADD34 levels were slightly elevated in the cells treated with these inhibitors,

which can be attributed to GCN2 activation. These results indicate that compounds LY-4 and GSK2656157 are inhibitors of PERK in multiple cell types. Furthermore, upon genetic ablation of PERK or pharmacological inhibition of PERK, GCN2 is suggested to be induced as a secondary eIF2 kinase.

Inhibition of PERK affects sphere formation of HCT116 cells in-vitro

We established that PERK is activated in response to anchorage-independent growth conditions and it has been proposed to promote cell survival during this process. To test the role of PERK activity during sphere development, soft agar assays were performed in the presence or absence of PERK inhibitors GSK2656157 and LY-4 and tumorsphere growth was compared to treatment with DMSO vehicle as a control. In this assay, single cells are suspended in a semi-solid gel like matrix such as agar or Matrigel. This assay better mimics the in-vivo anchorage-independent conditions. Each treatment sample was seeded in triplicates (3 wells per treatment) in a 24 well plate. HCT-116 cells were seeded into 24-well plates at 1000 cells per well mixed with 0.7% agar containing 2 µM of either inhibitor compound or vehicle DMSO. Normal growth media was layered on top of the agar matrix to ensure nutrient supply, along with same concentrations of compound or DMSO as in the agar layer. The assay was incubated at 37^{o}C and after 14 days, images of random fields of each well were captured at 10X magnification using an inverted compound microscope. The area of 90-95 spheres was measured using ImageJ software (as depicted in Figure 3 and Figure 6A) and the average area of spheres with PERK inhibitors was compared to DMSO control spheres. The spheres with PERK inhibitors had smaller area as compared to DMSO treated spheres (Figure 6B). The

number of spheres per field were also counted for PERK inhibited and DMSO control spheres. There was a statistically significant reduction ($p= 0.005$ and $p= 0.003$) in the number of spheres per field in wells treated with either GSK2656157 or LY-4 as compared to DMSO control (Figure 6C). These results, combined with those presented in figure 4, suggests that PERK activation is required for the growth of the tumorspheres. These results are consistent with findings by Bobrovnikova-Marjon E. et al, (45) suggesting that PERK is required for anchorage-independent growth of breast cancer cells. These results could be explained by a requirement for PERK activation in cancer cells growing in spheres to cope up with microenvironmental stresses such as hypoxia, oxidative stress, nutrient and glucose deprivation. Thus, targeting PERK activation may reduce the growth of tumor sphere of HCT116 cells.

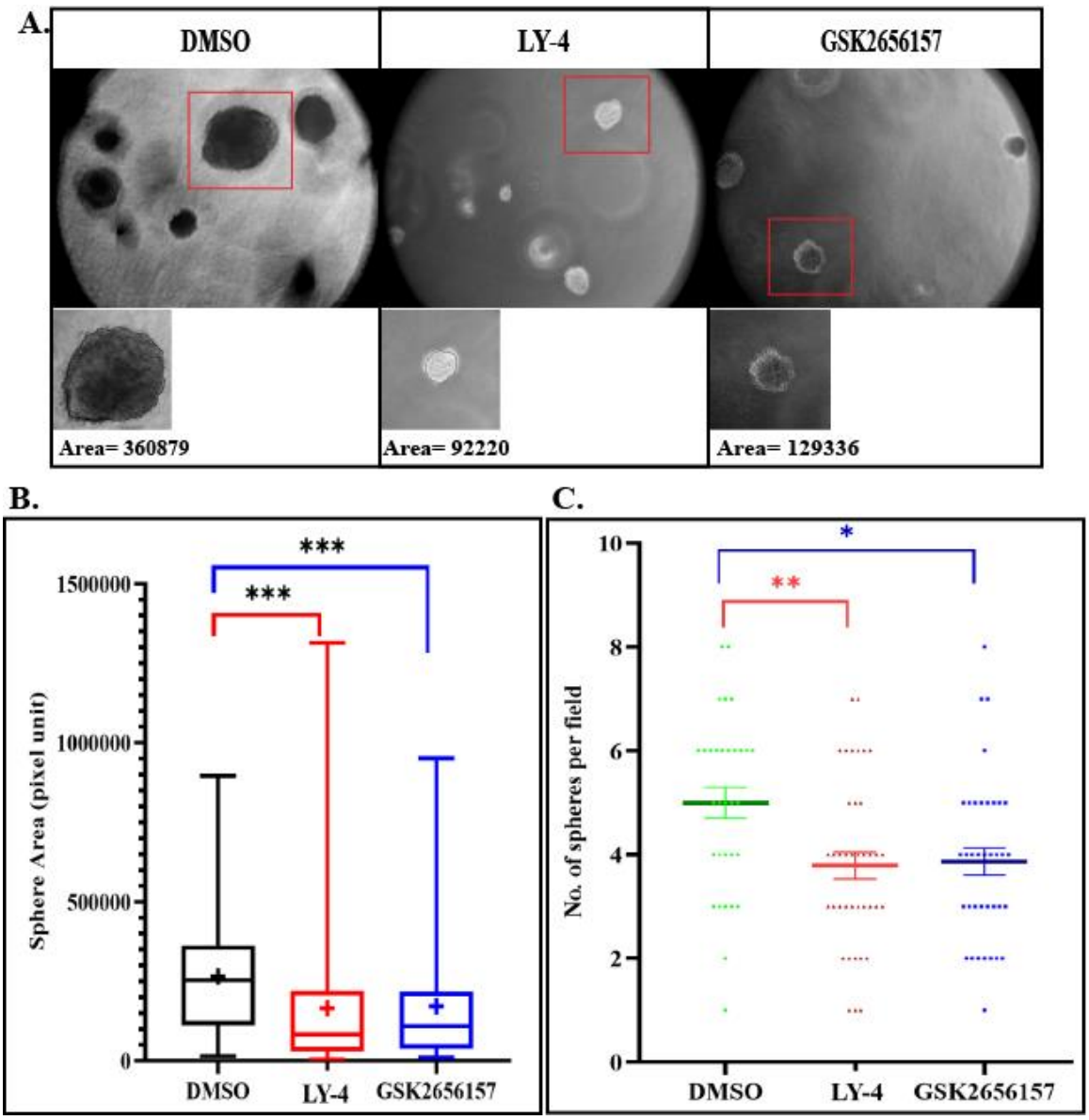

Figure 6: PERK inhibition reduces sphere formation in HCT116 cells in-vitro

A. Representative images of soft agar assay with HCT116 cells treated with PERK inhibitors LY-4 (2 µM) and GSK2656157 (2 µM) compared to DMSO control. Representative images of one sphere per field to demonstrate difference in size of sphere. Area measured in pixel units. B. Quantification of sphere area and difference in area when treated with inhibitor as compared to DMSO control. Statistical significance was determined by two-tailed student's T-test at $P<0.05$ and n= 90 to 95 spheres. "Horizontal

bar" in the box represents median, "+" represents mean, error bars represent maximum and minimum area of the spheres. C. Quantification of sphere count per field of soft agar assay treated with PERK inhibitor compared to DMSO control. Statistical significance in difference of spheres/field was determined by two-tailed student's T-test at $P<0.05$ and n=30 to 40 fields. *P=0.0055; **P=0.0033; *** P=0.001

PERK protein rather than its kinase activity is required for cell migration

To address whether PERK participates in cell migration, transwell migration assays were performed with treated MEF cells. Migration of wild type cells was compared with PERK knockout cells and wild type cells treated with PERK inhibitor GSK2656157. The MEF cells were seeded into culture inserts for a transwell migration assay. The cells were seeded in media without FBS in upper chamber and the media with FBS was added in the lower chamber (as depicted in figure 2) to stimulate cell migration. For wild-type and *PERK*$^{-/-}$ cells, normal growth media was used, whereas for inhibitor treatment 2 µM of GSK2656157 was added to the media in both the upper and lower chambers. Two membranes were seeded for every treatment condition. To record the amount of migration, inserts with cells were removed and fixed at 1 h, 6 h, 12 h and 18 h timepoints to measure the number of migrated cells. The insert membrane was removed and stained with DAPI and images of three random fields were captured per membrane and average cell count per field was determined as a measure of cell migration (Figure 7 A). All the cell counts per field were averaged and the difference in migration between wild type cells, those treated with inhibitor, and the *PERK*-deleted cells at each timepoint were analysed. There was a reduction in migration in the wild type cells upon treatment

with GSK2656157 that was only significant at 12 h (Figure 7 B). However, the *PERK*$^{-/-}$ knockout cells showed significant reduction in migration as compared to wild type cells throughout 18 h time course (Figure 7 C). These results suggest that PERK may facilitate early migration of these cells independent of its protein kinase activity.

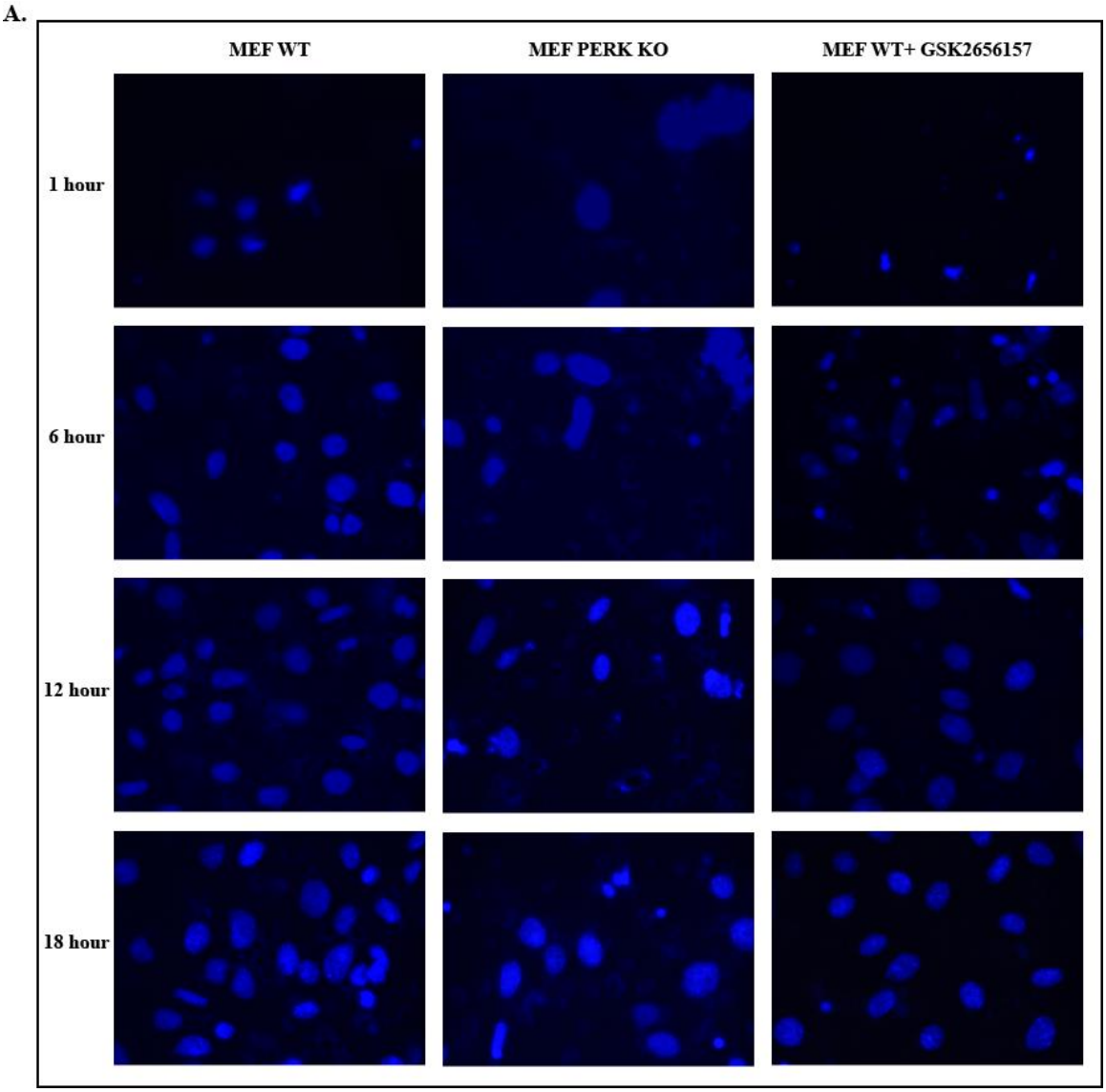

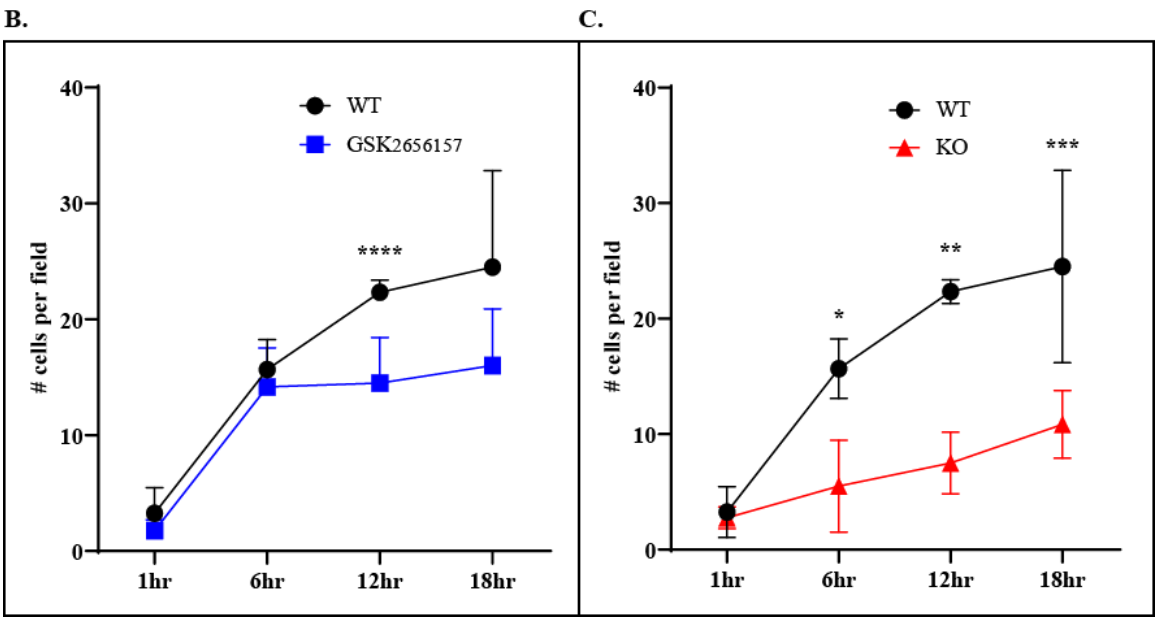

Figure 7: Knockout of *PERK* hinders transwell migration of MEF cells

A. Representation images of transwell cell migration of MEF cells. Pictures of a total of 6 fields were taken per treatment or genotype for each timepoint. Blue elliptical shapes of nucleus represent each cell, black apertures of the membrane pores in the background. B. Quantification of cell migration when treated with PERK inhibitor GSK2656157 compared to untreated wild type MEF cells. C. Quantification of cell migration of $PERK^{-/-}$ MEF cells compared to wild type MEF cells. Statistical significance in difference in cell migration at each timepoint was determined by two-tailed student's T-test at $P<0.05$ and n= 6 fields. *P=0.0003 **P<0.000001; ***P=0.0035; ****P=0.0008

DISCUSSION

From this study it was established that PERK is activated in anchorage-independent sphere formation of colorectal cancer cells in vitro and when PERK protein kinase activity is inhibited, the growth of sphere is hindered as verified by soft agar assays. Another potential role of PERK is in cell migration as demonstrated by ablation of PERK reducing transwell migration assay during a 18 h course. The role of PERK in migration may be more be as a scaffold protein rather than a protein kinase, as indicated by the difference in migration of *PERK*$^{-/-}$ cell versus the PERK inhibitor treated MEF cells.

PERK has been shown to be activated in anchorage- independent culture conditions by a number of stress conditions including autophagy, hypoxia, DNA damage, and ROS production (48-50). In this study, the soft agar assay (Figure 6) showed that PERK protein kinase activity is required for sphere formation, consistent with its role as a UPR component. Overall, the role of PERK in anchorage-independence suggest that it is a good target for developing anti-cancer therapies. Lowering the chances of survival of cancer cells in anchorage-independent growth may reduce the rate of metastasis and improve the treatment of patients. However, the results noted in this study should be analyzed further to address which additional cellular stress conditions activate PERK. Following up with this study, the role of PERK in anchorage- independent growth and eventually in metastasis needs to be addressed using in-vivo experiments with specific PERK inhibitors to determine its definitive use in anti-cancer treatment.

Another finding of this study was a role for PERK in cell migration. Genetic deletion of PERK significantly hindered cell migration (Figure 7). By contrast, pharmacological inhibition of PERK protein kinase activity did not block migration of cells. These results suggest that PERK may serve as a scaffold protein providing for migration function via protein-protein interactions. The *PERK*$^{-/-}$ cells lacked part of the luminal domain, transmembrane domain, and part of the catalytic domain of majority of PERK protein synthesized. Any partial protein produced would not be stable or abundantly expressed. So, the parts of these domain lacking in PERK$^{-/-}$ cells may contribute to cell migration. The GSK2656157 inhibitor also shows some off-target effects, which might be interfering with PERK inhibition. Collectively, PERK is an essential protein for cell migration, although which domain of the protein is essential for it could not be determined. To establish the role of PERK in migration, more repetitive results and direct proof need to be established. To accomplish that, the migration experiment could be repeated with different deletions in *PERK* gene to compare which deletions affect the migration the most. Or an immunofluorescent staining of migrating cells can be done to determine changes in cytoskeleton during presence, absence of *PERK* or pharmacological inhibition of PERK.

Recent studies also indicate a key role of UPR members, PERK and IRE1α, in cell migration. Consistent with the results in this study, van Vliet A. R. et al (59) showed that PERK knockout changes the cytoskeleton of the cell and makes the cells defective in migration. When rescued by full length kinase dead PERK, their migration abilities were

almost restored to the levels observed for expression of wild-type PERK. The results from the studies detailed above indicates that the mere presence of PERK is required for normal cell migration irrespective of its kinase activity. Whereas, findings from other groups suggest that PERK is activated in cancer cells and facilitates cell migration through various downstream effectors such as MALAT1, LAMP3 and CREB3L1 via UPR cascade (44,54,55).

In conclusion, unfolded protein response is a survival mechanism for the cells during stress conditions. But the cancer cells exploit this survival mechanism for their benefit- to survive various intrinsic and extrinsic stresses via UPR and ISR components. The involvement of UPR/ISR members in cancer cell survival makes them a great target for anti-cancer therapies. The role of PERK in cancer progression and metastasis is not fully explored, but the outcomes from existing studies certainly make it a target worth pursuing in the future.

REFERENCES

1. Almanza, A., Carlesso, A., Chintha, C., Creedican, S., Doultsinos, D., Leuzzi, B., Luis, A., McCarthy, N., Montibeller, L., More, S., Papaioannou, A., Puschel, F., Sassano, M. L., Skoko, J., Agostinis, P., de Belleroche, J., Eriksson, L. A., Fulda, S., Gorman, A. M., Healy, S., Kozlov, A., Munoz-Pinedo, C., Rehm, M., Chevet, E., and Samali, A. (2019) Endoplasmic reticulum stress signalling - from basic mechanisms to clinical applications. *FEBS J* **286**, 241-278

2. Banerjee, A., Banerjee, V., Czinn, S., and Blanchard, T. (2017) Increased reactive oxygen species levels cause ER stress and cytotoxicity in andrographolide treated colon cancer cells. *Oncotarget* **8**, 26142-26153

3. Grigaravicius, P., Kaminska, E., Hubner, C. A., McKinnon, P. J., von Deimling, A., and Frappart, P. O. (2016) Rint1 inactivation triggers genomic instability, ER stress and autophagy inhibition in the brain. *Cell Death Differ* **23**, 454-468

4. Koumenis, C., Naczki, C., Koritzinsky, M., Rastani, S., Diehl, A., Sonenberg, N., Koromilas, A., and Wouters, B. G. (2002) Regulation of protein synthesis by hypoxia via activation of the endoplasmic reticulum kinase PERK and phosphorylation of the translation initiation factor eIF2alpha. *Mol Cell Biol* **22**, 7405-7416

5. Xu, X., Gupta, S., Hu, W., McGrath, B. C., and Cavener, D. R. (2011) Hyperthermia induces the ER stress pathway. *PLoS One* **6**, e23740

6. Thastrup O, C. P., Drøbak BK, Hanley MR,, and AP, D. (1990) Thapsigargin, a tumor promoter, discharges intracellular Ca2+ stores by specific inhibition of the endoplasmic reticulum Ca2+ ATPase. *Proc Natl Acad Sci USA* **87**, 2466–2470

7. Oslowski, C. M., and Urano, F. (2011) Measuring ER stress and the unfolded protein response using mammalian tissue culture system. *Methods Enzymol* **490**, 71-92

8. Bertolotti A., Z. Y., Linda M. Hendershot L., Heather P. Harding & David Ron. (2000) Dynamic interaction of BiP and ER stress transducers in the unfolded-protein response. *Nat Cell Biol* **2**, 326-332

9. Baird, T. D., and Wek, R. C. (2012) Eukaryotic initiation factor 2 phosphorylation and translational control in metabolism. *Adv Nutr* **3**, 307-321

10. Wek, R. C. (2018) Role of eIF2alpha Kinases in Translational Control and Adaptation to Cellular Stress. *Cold Spring Harb Perspect Biol* **10**

11. Walter, B. M. G. a. P. (2011) Unfolded Proteins are Ire1-Activating Ligands that Directly Induce the Unfolded Protein Response. *Science* **333**, 1891-1894

12. Cui, W., Li, J., Ron, D., and Sha, B. (2011) The structure of the PERK kinase domain suggests the mechanism for its activation. *Acta Crystallogr D Biol Crystallogr* **67**, 423-428

13. Jurkin, J., Henkel, T., Nielsen, A. F., Minnich, M., Popow, J., Kaufmann, T., Heindl, K., Hoffmann, T., Busslinger, M., and Martinez, J. (2014) The

mammalian tRNA ligase complex mediates splicing of XBP1 mRNA and controls antibody secretion in plasma cells. *EMBO J* **33**, 2922-2936

14. Chang, T. K., Lawrence, D. A., Lu, M., Tan, J., Harnoss, J. M., Marsters, S. A., Liu, P., Sandoval, W., Martin, S. E., and Ashkenazi, A. (2018) Coordination between Two Branches of the Unfolded Protein Response Determines Apoptotic Cell Fate. *Mol Cell* **71**, 629-636 e625

15. Shi, Y., Vattem, K. M., Sood, R., An, J., Liang, J., Stramm, L., and Wek, R. C. (1998) Identification and characterization of pancreatic eukaryotic initiation factor 2 alpha-subunit kinase, PEK, involved in translational control. *Mol Cell Biol* **18**, 7499-7509

16. Harding, H. P., Zhang, Y., and Ron, D. (1999) Protein translation and folding are coupled by an endoplasmic-reticulum-resident kinase. *Nature* **397**, 271-274

17. Cullinan, S. B., Zhang, D., Hannink, M., Arvisais, E., Kaufman, R. J., and Diehl, J. A. (2003) Nrf2 is a direct PERK substrate and effector of PERK-dependent cell survival. *Mol Cell Biol* **23**, 7198-7209

18. Bobrovnikova-Marjon, E., Pytel, D., Riese, M. J., Vaites, L. P., Singh, N., Koretzky, G. A., Witze, E. S., and Diehl, J. A. (2012) PERK utilizes intrinsic lipid kinase activity to generate phosphatidic acid, mediate Akt activation, and promote adipocyte differentiation. *Mol Cell Biol* **32**, 2268-2278

19. Zhang, W., Hietakangas, V., Wee, S., Lim, S. C., Gunaratne, J., and Cohen, S. M. (2013) ER stress potentiates insulin resistance through PERK-mediated FOXO phosphorylation. *Genes Dev* **27**, 441-449

20. Wek, R. C., Jackson, B. M., and Hinnebusch, A. G. (1989) Juxtaposition of domains homologous to protein kinases and histidyl-tRNA synthetases in GCN2 protein suggests a mechanism for coupling GCN4 expression to amino acid availability. *Proc Natl Acad Sci U S A* **86**, 4579-4583

21. Jing Deng, H. P. H., Brian Raught, Anne-Claude Gingras, Juan Jose Berlanga, Donalyn Scheuner, Randal J. Kaufman, David Ron and Nahum Sonenberg. (2002) Activation of GCN2 in UV-Irradiated Cells Inhibits Translation. *Current Biology* **12**, 1279-1286

22. Burwick, N., and Aktas, B. H. (2017) The eIF2-alpha kinase HRI: a potential target beyond the red blood cell. *Expert Opin Ther Targets* **21**, 1171-1177

23. Xiaoyan Guo, G. A., Yi Liu, Ruilin Tian, Bret A. Unger, Yu-Hsiu T. Lin, Arun P. Wiita, Ke Xu, M. Almira Correia and Martin Kampmann. (2020) Mitochondrial stress is relayed to the cytosol by an OMA1–DELE1–HRI pathway. *Nature* **579**, 427-432

24. Fessler, E., Eckl, E. M., Schmitt, S., Mancilla, I. A., Meyer-Bender, M. F., Hanf, M., Philippou-Massier, J., Krebs, S., Zischka, H., and Jae, L. T. (2020) A pathway coordinated by DELE1 relays mitochondrial stress to the cytosol. *Nature* **579**, 433-437

25. Katze, M. G., Wambach, M., Wong, M. L., Garfinkel, M., Meurs, E., Chong, K., Williams, B. R., Hovanessian, A. G., and Barber, G. N. (1991) Functional expression and RNA binding analysis of the interferon-induced, double-stranded RNA-activated, 68,000-Mr protein kinase in a cell-free system. *Mol Cell Biol* **11**, 5497-5505

26. Harding, H. P., Zhang, Y., Zeng, H., Novoa, I., Lu, P. D., Calfon, M., Sadri, N., Yun, C., Popko, B., Paules, R., Stojdl, D. F., Bell, J. C., Hettmann, T., Leiden, J. M., and Ron, D. (2003) An integrated stress response regulates amino acid metabolism and resistance to oxidative stress. *Mol Cell* **11**, 619-633

27. Vattem, K. M., and Wek, R. C. (2004) Reinitiation involving upstream ORFs regulates ATF4 mRNA translation in mammalian cells. *Proc Natl Acad Sci U S A* **101**, 11269-11274

28. Harding, H. P., Novoa, I., Zhang, Y., Zeng, H., Wek, R., Schapira, M., and Ron, D. (2000) Regulated translation initiation controls stress-induced gene expression in mammalian cells. *Mol Cell* **6**, 1099-1108

29. Novoa, I., Zeng, H., Harding, H. P., and Ron, D. (2001) Feedback inhibition of the unfolded protein response by GADD34-mediated dephosphorylation of eIF2alpha. *J Cell Biol* **153**, 1011-1022

30. Baird, T. D., Palam, L. R., Fusakio, M. E., Willy, J. A., Davis, C. M., McClintick, J. N., Anthony, T. G., and Wek, R. C. (2014) Selective mRNA translation during

eIF2 phosphorylation induces expression of IBTKalpha. *Mol Biol Cell* **25**, 1686-1697

31. Palam, L. R., Baird, T. D., and Wek, R. C. (2011) Phosphorylation of eIF2 facilitates ribosomal bypass of an inhibitory upstream ORF to enhance CHOP translation. *J Biol Chem* **286**, 10939-10949

32. Ma, Y., and Hendershot, L. M. (2003) Delineation of a negative feedback regulatory loop that controls protein translation during endoplasmic reticulum stress. *J Biol Chem* **278**, 34864-34873

33. Lee, Y. Y., Cevallos, R. C., and Jan, E. (2009) An upstream open reading frame regulates translation of GADD34 during cellular stresses that induce eIF2alpha phosphorylation. *J Biol Chem* **284**, 6661-6673

34. Young, S. K., Willy, J. A., Wu, C., Sachs, M. S., and Wek, R. C. (2015) Ribosome Reinitiation Directs Gene-specific Translation and Regulates the Integrated Stress Response. *J Biol Chem* **290**, 28257-28271

35. Brush, M. H., Weiser, D. C., and Shenolikar, S. (2003) Growth arrest and DNA damage-inducible protein GADD34 targets protein phosphatase 1 alpha to the endoplasmic reticulum and promotes dephosphorylation of the alpha subunit of eukaryotic translation initiation factor 2. *Mol Cell Biol* **23**, 1292-1303

36. Connor, J. H., Weiser, D. C., Li, S., Hallenbeck, J. M., and Shenolikar, S. (2001) Growth arrest and DNA damage-inducible protein GADD34 assembles a novel

signaling complex containing protein phosphatase 1 and inhibitor 1. *Mol Cell Biol* **21**, 6841-6850

37. Novoa, I., Zhang, Y., Zeng, H., Jungreis, R., Harding, H. P., and Ron, D. (2003) Stress-induced gene expression requires programmed recovery from translational repression. *EMBO J* **22**, 1180-1187

38. Piwocka, K., Vejda, S., Cotter, T. G., O'Sullivan, G. C., and McKenna, S. L. (2006) Bcr-Abl reduces endoplasmic reticulum releasable calcium levels by a Bcl-2-independent mechanism and inhibits calcium-dependent apoptotic signaling. *Blood* **107**, 4003-4010

39. Staschke, K. A., and Wek, R. C. (2019) Adapting to cell stress from inside and out. *Nat Cell Biol* **21**, 799-800

40. Nguyen, H. G., Conn, C. S., Kye, Y., Xue, L., Forester, C. M., Cowan, J. E., Hsieh, A. C., Cunningham, J. T., Truillet, C., Tameire, F., Evans, M. J., Evans, C. P., Yang, J. C., Hann, B., Koumenis, C., Walter, P., Carroll, P. R., and Ruggero, D. (2018) Development of a stress response therapy targeting aggressive prostate cancer. *Sci Transl Med* **10**

41. Hart, L. S., Cunningham, J. T., Datta, T., Dey, S., Tameire, F., Lehman, S. L., Qiu, B., Zhang, H., Cerniglia, G., Bi, M., Li, Y., Gao, Y., Liu, H., Li, C., Maity, A., Thomas-Tikhonenko, A., Perl, A. E., Koong, A., Fuchs, S. Y., Diehl, J. A., Mills, I. G., Ruggero, D., and Koumenis, C. (2012) ER stress-mediated autophagy

promotes Myc-dependent transformation and tumor growth. *J Clin Invest* **122**, 4621-4634

42. Bi, M., Naczki, C., Koritzinsky, M., Fels, D., Blais, J., Hu, N., Harding, H., Novoa, I., Varia, M., Raleigh, J., Scheuner, D., Kaufman, R. J., Bell, J., Ron, D., Wouters, B. G., and Koumenis, C. (2005) ER stress-regulated translation increases tolerance to extreme hypoxia and promotes tumor growth. *EMBO J* **24**, 3470-3481

43. Blais, J. D., Addison, C. L., Edge, R., Falls, T., Zhao, H., Wary, K., Koumenis, C., Harding, H. P., Ron, D., Holcik, M., and Bell, J. C. (2006) Perk-dependent translational regulation promotes tumor cell adaptation and angiogenesis in response to hypoxic stress. *Mol Cell Biol* **26**, 9517-9532

44. Nagelkerke, A., Bussink, J., Mujcic, H., Wouters, B. G., Lehmann, S., Sweep, F. C., and Span, P. N. (2013) Hypoxia stimulates migration of breast cancer cells via the PERK/ATF4/LAMP3-arm of the unfolded protein response. *Breast Cancer Res* **15**, R2

45. Bobrovnikova-Marjon, E., Grigoriadou, C., Pytel, D., Zhang, F., Ye, J., Koumenis, C., Cavener, D., and Diehl, J. A. (2010) PERK promotes cancer cell proliferation and tumor growth by limiting oxidative DNA damage. *Oncogene* **29**, 3881-3895

46. Salaroglio, I. C., Panada, E., Moiso, E., Buondonno, I., Provero, P., Rubinstein, M., Kopecka, J., and Riganti, C. (2017) PERK induces resistance to cell death elicited by endoplasmic reticulum stress and chemotherapy. *Mol Cancer* **16**, 91

47. Friedl, P., and Wolf, K. (2003) Proteolytic and non-proteolytic migration of tumour cells and leucocytes. *Biochem Soc Symp*, 277-285

48. Paoli, P., Giannoni, E., and Chiarugi, P. (2013) Anoikis molecular pathways and its role in cancer progression. *Biochim Biophys Acta* **1833**, 3481-3498

49. Taddei, M. L., Giannoni, E., Fiaschi, T., and Chiarugi, P. (2012) Anoikis: an emerging hallmark in health and diseases. *J Pathol* **226**, 380-393

50. Avivar-Valderas, A., Salas, E., Bobrovnikova-Marjon, E., Diehl, J. A., Nagi, C., Debnath, J., and Aguirre-Ghiso, J. A. (2011) PERK integrates autophagy and oxidative stress responses to promote survival during extracellular matrix detachment. *Mol Cell Biol* **31**, 3616-3629

51. Fares, J., Fares, M. Y., Khachfe, H. H., Salhab, H. A., and Fares, Y. (2020) Molecular principles of metastasis: a hallmark of cancer revisited. *Signal Transduct Target Ther* **5**, 28

52. Sun, B. O., Fang, Y., Li, Z., Chen, Z., and Xiang, J. (2015) Role of cellular cytoskeleton in epithelial-mesenchymal transition process during cancer progression. *Biomed Rep* **3**, 603-610

53. Zeng, P., Sun, S., Li, R., Xiao, Z. X., and Chen, H. (2019) HER2 Upregulates ATF4 to Promote Cell Migration via Activation of ZEB1 and Downregulation of E-Cadherin. *Int J Mol Sci* **20**

54. Jiang, X., Li, D., Wang, G., Liu, J., Su, X., Yu, W., Wang, Y., Zhai, C., Liu, Y., and Zhao, Z. (2020) Thapsigargin promotes colorectal cancer cell migration through upregulation of lncRNA MALAT1. *Oncol Rep* **43**, 1245-1255

55. Feng, Y. X., Jin, D. X., Sokol, E. S., Reinhardt, F., Miller, D. H., and Gupta, P. B. (2017) Cancer-specific PERK signaling drives invasion and metastasis through CREB3L1. *Nat Commun* **8**, 1079

56. Alert R., T. X. (2020) Physical Models of Collective Cell Migration. *Annual Review of Condensed Matter Physics* **11**, 77-101

57. Tojkander, S., Gateva, G., and Lappalainen, P. (2012) Actin stress fibers--assembly, dynamics and biological roles. *J Cell Sci* **125**, 1855-1864

58. Urra, H., Henriquez, D. R., Canovas, J., Villarroel-Campos, D., Carreras-Sureda, A., Pulgar, E., Molina, E., Hazari, Y. M., Limia, C. M., Alvarez-Rojas, S., Figueroa, R., Vidal, R. L., Rodriguez, D. A., Rivera, C. A., Court, F. A., Couve, A., Qi, L., Chevet, E., Akai, R., Iwawaki, T., Concha, M. L., Glavic, A., Gonzalez-Billault, C., and Hetz, C. (2018) IRE1alpha governs cytoskeleton remodelling and cell migration through a direct interaction with filamin A. *Nat Cell Biol* **20**, 942-953

59. van Vliet, A. R., Giordano, F., Gerlo, S., Segura, I., Van Eygen, S., Molenberghs, G., Rocha, S., Houcine, A., Derua, R., Verfaillie, T., Vangindertael, J., De Keersmaecker, H., Waelkens, E., Tavernier, J., Hofkens, J., Annaert, W., Carmeliet, P., Samali, A., Mizuno, H., and Agostinis, P. (2017) The ER Stress Sensor PERK Coordinates ER-Plasma Membrane Contact Site Formation through Interaction with Filamin-A and F-Actin Remodeling. *Mol Cell* **65**, 885-899 e886

60. Jiang, H. Y., Wek, S. A., McGrath, B. C., Lu, D., Hai, T., Harding, H. P., Wang, X., Ron, D., Cavener, D. R., and Wek, R. C. (2004) Activating transcription factor 3 is integral to the eukaryotic initiation factor 2 kinase stress response. *Mol Cell Biol* **24**, 1365-1377

61. Teske, B. F., Wek, S. A., Bunpo, P., Cundiff, J. K., McClintick, J. N., Anthony, T. G., and Wek, R. C. (2011) The eIF2 kinase PERK and the integrated stress response facilitate activation of ATF6 during endoplasmic reticulum stress. *Mol Biol Cell* **22**, 4390-4405

62. Tenkerian, C., Krishnamoorthy, J., Mounir, Z., Kazimierczak, U., Khoutorsky, A., Staschke, K. A., Kristof, A. S., Wang, S., Hatzoglou, M., and Koromilas, A. E. (2015) mTORC2 Balances AKT Activation and eIF2alpha Serine 51 Phosphorylation to Promote Survival under Stress. *Mol Cancer Res* **13**, 1377-1388

63. Moscona, J. F. A. (1978) Role of cell shape in growth control. *Nature* **273**, 345-349

64. Fukazawa H, M. S., Uehara Y. (1995) A microplate assay for quantification of anchorage-independent growth of transformed cells. *Anal Biochem* **228**, 83-90

65. Schneider, C. A., Rasband, W. S., and Eliceiri, K. W. (2012) NIH Image to ImageJ: 25 years of image analysis. *Nat Methods* **9**, 671-675

66. Keller, T. L., Zocco, D., Sundrud, M. S., Hendrick, M., Edenius, M., Yum, J., Kim, Y. J., Lee, H. K., Cortese, J. F., Wirth, D. F., Dignam, J. D., Rao, A., Yeo, C. Y., Mazitschek, R., and Whitman, M. (2012) Halofuginone and other febrifugine derivatives inhibit prolyl-tRNA synthetase. *Nat Chem Biol* **8**, 311-317

67. Axten, J. M., Romeril, S. P., Shu, A., Ralph, J., Medina, J. R., Feng, Y., Li, W. H., Grant, S. W., Heerding, D. A., Minthorn, E., Mencken, T., Gaul, N., Goetz, A., Stanley, T., Hassell, A. M., Gampe, R. T., Atkins, C., and Kumar, R. (2013) Discovery of GSK2656157: An Optimized PERK Inhibitor Selected for Preclinical Development. *ACS Med Chem Lett* **4**, 964-968

68. Atkins, C., Liu, Q., Minthorn, E., Zhang, S. Y., Figueroa, D. J., Moss, K., Stanley, T. B., Sanders, B., Goetz, A., Gaul, N., Choudhry, A. E., Alsaid, H., Jucker, B. M., Axten, J. M., and Kumar, R. (2013) Characterization of a novel PERK kinase inhibitor with antitumor and antiangiogenic activity. *Cancer Res* **73**, 1993-2002

69. Rojas-Rivera, D., Delvaeye, T., Roelandt, R., Nerinckx, W., Augustyns, K., Vandenabeele, P., and Bertrand, M. J. M. (2017) When PERK inhibitors turn out to be new potent RIPK1 inhibitors: critical issues on the specificity and use of GSK2606414 and GSK2656157. *Cell Death Differ* **24**, 1100-1110

70. Dariusz Pytel, Y. G., Katarzyna Mackiewicz,Yuliya V. Katlinskaya, Kirk A. Staschke, Maria C. G. Paredes, Akihiro Yoshida, Shuo Qie, Gao Zhang, Olga S. Chajewski, Lawrence Wu, Ireneusz Majsterek, Meenhard Herlyn, Serge Y. Fuchs, J. Alan Diehl (2016) PERK Is a Haploinsufficient Tumor Suppressor: Gene Dose Determines Tumor-Suppressive Versus Tumor Promoting Properties of PERK in Melanoma. *PLOS Genetics* **12: e1006518**

71. Tameire, F., Verginadis, II, Leli, N. M., Polte, C., Conn, C. S., Ojha, R., Salas Salinas, C., Chinga, F., Monroy, A. M., Fu, W., Wang, P., Kossenkov, A., Ye, J., Amaravadi, R. K., Ignatova, Z., Fuchs, S. Y., Diehl, J. A., Ruggero, D., and Koumenis, C. (2019) ATF4 couples MYC-dependent translational activity to bioenergetic demands during tumour progression. *Nat Cell Biol* **21**, 889-899

CURRICULUM VITAE

Madhura Shirish Shukla

Education:

Indiana University (IUPUI), Indianapolis, USA **2018-2020**

Master of Science, Biochemistry and Molecular Biology

GPA: 3.75/4.00

University of Mumbai, Mumbai, India **2017-2018**

Master of Science, Biotechnology (2 semesters, 48 credits)

GPA: 8.42/10.00 | Grade: A

University of Mumbai, Mumbai, India **2014-2017**

Bachelor of Science, Biotechnology

GPA: 6.67/7.00 | Grade: A

Projects:

Role of PERK in Anchorage- Independent Growth of Colorectal Carcinoma and Cell Migration In-Vitro

November 2018- July 2020

Master's student, Dr. Wek Lab, IUPUI

- Maintained and cultured human cancer cell line as adherent & suspension culture in BSL2 cabinet.

- Established stable mammalian cell line after virus mediated delivery of cloned genes and CRISPR Knockout; analysed using western blot and DNA sequencing.
- Modified, optimized, and tested protocols for soft agar assay and trans-well cell migration assay; then used them as in-vitro cancer study model.
- Recorded, analyzed and compiled the data collected from experiments using appropriate software.

Analysis and Applications of Essential Oil from *Cymbopogon citratus* (Lemongrass)

December 2016- February 2017

Bachelor's student, Dept. of Biotechnology, V.G. Vaze College, Mumbai

- Operated steam distillation apparatus to isolate essential oil.
- Analysed and interpreted the GC-MS results of the isolated essential oil.
- Formulated cosmetic products using the essential oils based on their medicinal properties.

Bacteriological examination of street foods (liquids)

May 2016

Bachelor's student, Dept. of Biotechnology, V.G. Vaze College, Mumbai

- Collected samples from various street food outlets.
- Performed bacteriological analysis of samples with aseptic microbiological techniques.

- Used three techniques, namely- MPN method for bacterial load, selective media, Gram staining for analysis.
- Presented a poster at college level competition in the academic year of 2016-17.